9199407110001

LARGE-SCALE BUOYANT FLOW AT AN UNSATURATED HLW REPOSITORY

R. D. Manteufel
Center for Nuclear Waste Regulatory Analyses
San Antonio, TX

ABSTRACT

A simplified model is developed for thermally-driven buoyant gas flow in an unsaturated repository such as that anticipated at Yucca Mountain. Based on a simplified thermosyphon model, the magnitude of buoyant gas flow is related to key thermal-hydraulic parameters (e.g., bulk permeability and maximum repository temperature). The effects of buoyant gas flow on vapor flow and heat transport near the repository horizon are assessed, namely: (i) the magnitude of buoyant flow through the repository, (ii) the effect of buoyant flow on vapor transfer, and (iii) the effect of buoyant flow on heat transfer.

NOMENCLATURE

A	cross-sectional area of thermosyphon [m^2]
A_{up}	cross-sectional area of the thermosyphon in upward-flowing hot leg [m^2]
D	effective porous medium diffusion coefficient [~10^{-6} m^2/s]
F_{visc}	viscous force acting on gas [N]
F_{buoy}	buoyant force acting on gas [N]
g	gravitational constant (9.81m/s^2)
h_{fg}	enthalpy of vaporization (~2.4 10^6 J/kg)
$j_{e,cond}$	conductive energy flux in the rock mass [W/m^2]
$j_{e,w,g}$	conductive energy flux due to latent heat of vapor [W/m^2]
$j_{m,w,g}$	diffusive mass flux of water in the gas phase [kg/(m^2-s)]
k_b	bulk gas permeability of rock mass [m^2]
k_{rock}	thermal conductivity of rock mass [~2 W/(m-C)]
ℓ	length along thermosyphon [m]
L	length scale (see Figure 1) [m]
M_w	molecular weight of water (18 kg/kmole)
Pe	Peclet number [-], $Pe = \frac{u\ L}{D}$
P_g	total gas pressure [N/m^2]
P_v	vapor pressure of water [N/m^2]
R	ideal gas constant [8314 J/(kmole-K)]
S_l	liquid saturation (m^3 liquid/ m^3 void) [-]
S_g	gas saturation (m^3 gas/ m^3 void) [-]
t	time [s]
T	temperature [K]
T_o	reference temperature [K]
T_m	maximum temperature [K]
ΔT	change in temperature from the reference [K]
ΔT_m	maximum increase in temperature [K]
u	area-average (Darcy) velocity [m/s]
Vp	vapor pressure number [-], $Vp = \frac{h_{fg} M_w}{R T^2} \Delta T_m$
$q_{e,w,g}$	advective energy flux due to latent heat of vapor [W/m^2]
$q_{m,g}$	advective mass flux of the gas [kg/(m^2-s)]
$q_{m,w,\ell}$	advective mass flux of liquid water [kg/(m^2-s)]
$q_{m,w,g}$	advective mass flux of water vapor [kg/(m^2-s)]
q_{src}	areal heat source due to radioactive decay [W/m^2]
$Q_{c/v}$	condensation/vaporization term [kg/(m^3-s)]
$\hat{Q}_{c/v}$	dimensionless condensation/vaporization term, $\hat{Q}_{c/v} = \frac{Q_{c/v}}{\left[\frac{\rho_o D}{L^2}(Vp)^2\right]}$
z	elevation [m]

$\hat{z}$ dimensionless elevation, $\hat{z} = \frac{z}{L}$

α thermal diffusivity [m^2/s]

β volumetric expansion coef. for ideal gas [1/K]

ρ bulk gas density [kg/m^3]

$(\rho c)_{rock}$ density times specific heat of rock [~$2x10^6$ J/m^3-C]

ρ_o reference vapor density [kg/m^3]

ρ_ℓ liquid density [kg/m^3]

ρ_v density of water vapor which is a function of temperature [kg/m^3]

τ time constant [s]

ϕ porosity (m^3 void/ m^3 medium) [-]

θ dimensionless temperature, $\theta = \frac{\Delta T}{\Delta T_m}$

ν kinematic viscosity of gas [m^2/s]

INTRODUCTION

Previous studies have been directed at developing an understanding of the effects of decay heat from high-level waste (HLW) on the subsequent gas flow and the redistribution of *in situ* groundwater (Wang et. al., 1983; Pollock, 1986; Rajen and Kulacki, 1987; Pruess et. al., 1990a,1990b; Rajen, 1989; Amter and Ross, 1991; Buscheck and Nitao 1992, 1993; Manteufel and Green, 1993). It has been noted that large-scale (of the order of kilometers) buoyant gas flow patterns may develop in the geologic medium. Consequences of buoyant gas flows include accelerating the transport of volatile radionuclides and potentially leading to the formation of temporary "perched" zones of groundwater (which may subsequently lead to increased and sustained groundwater seepage through saturated paths). A number of similarities have been identified in the results of earlier investigations, namely that the buoyant gas flow patterns lead to upward-directed gas flow through the repository horizon. Although the gas flow patterns can be complicated due to the geometrically complex topographic and stratigraphic effects (Amter and Ross, 1991), this effort is a continuation of our efforts (Manteufel and Powell, 1994) to develop a simple model that captures the fundamental flow pattern. We intend to use the simplified model to determine the dominant scaling relationships and identify important phenomena. These results can be used to complement and guide more complex numerical simulations.

BUOYANT THERMOSYPHON

The repository is modeled as a disk-shaped heat source located halfway between the ground surface and the water table. The ground (i.e., rock) is assumed to be a homogeneous porous medium and buoyancy-driven gas streamlines are assumed to develop as illustrated in Figure 1. The assumed pattern of the streamlines is based on the results of earlier works (Wang et. al., 1983; Pollock, 1986; Amter and Ross, 1991; Buscheck and Nitao 1992, 1993). It is very probable that at early times, the gas flow patterns are not as assumed in Figure 1, but have a transient pattern that can be different from the final flow pattern (Rajen and Kulacki, 1987). Also, the presence of a layered, heterogeneous medium is expected to effect the actual flow pattern (Amter and Ross, 1991). However, a simplified model is adopted here to understand the cause-and-effect relationships which govern buoyant gas flow, and allow a quantification of buoyancy effects on heat and moisture transfer.

A thermospyhon is defined as a streamtube which: (i) begins at the ground surface at a distance away from the repository, (ii) travels downwards toward the water table and below the repository, and finally (iii) travels upwards through the repository before exiting at the ground surface above the repository. The thermosyphon has two distinct legs: a cool, downward-directed leg and a hot, upward-directed leg. In the hot leg, bulk gas motion is a result of a combination of gravity and temperature-induced density variations in the gas. Viscous forces develop as the gas flows through the porous geologic medium. The thermosyphon model is essentially one-dimensional (along the stream line) and is used to establish the relationship between the buoyant driving force and the upward gas velocity through the repository. The gas flow inside the thermosyphon is assumed to obey Darcy's law which assumes the inertia of the flow is negligible. Because the gas flow has negligible momentum, the gas flow responds rapidly to changes in the temperature field. The buoyant gas flow field changes much quickly than the temperature field, hence it is justifiable to assume the buoyant gas flow is in quasi-static equilibrium with the instantaneous temperature field. The quasi-static nature of the gas flow indicates that the buoyant and viscous forces are always equal and opposite for a given time.

The thermosyphon analysis is based on a balance of the temperature-induced buoyant force and the flow-induced viscous force (where the momentum of a fluid flowing in a porous medium is considered to be negligible). Because the flow is assumed to be quasi-static equilibrium, the balance of forces is true at every point in time.

$$F_{visc} + F_{buoy} = 0 \qquad (1)$$

In Eq 1, the boiling driving force is omitted because it has not been successfully included in this simple model. This work is being extended to investigate the effect of having the maximum temperature exceed the boiling temperature. Each of these terms are developed next. A list of nomenclature is included at the beginning of the paper.

Viscous Force

The advective mass flux of the gas is related to the gas pressure gradient through Darcy's law.

$$\vec{q}_{m,g} = -\frac{k_b}{\nu}\frac{dP_g}{d\ell}\vec{\ell} \qquad (2)$$

Pressure times area is equal to force, hence for convenience Darcy's law is re-expressed as

$$\frac{d\vec{F}_{visc}}{d\ell} = -\frac{\rho_o A}{(k_b/\nu)}\vec{u} \qquad (3)$$

The net dynamic viscous force can be obtained by integrating the gradient around the length of the thermosyphon.

$$F_{visc} = \oint_{streamline}\frac{d\vec{F}_{visc}}{d\ell}\bullet d\vec{\ell} = -\oint\frac{\rho_o A}{(k_b/\nu)}\vec{u}\bullet d\vec{\ell} \qquad (4)$$

The mass flow rate is constant throughout the thermosyphon (neglecting the vaporization/condensation of groundwater which will be considered later in the paper). Hence the term ($\rho A u$), is constant throughout the thermosyphon. For the conservation of mass, the gas density is approximately constant, $\rho \cong \rho_o$. Because we are interested in the upward gas velocity through the repository, Eq 4 is evaluated in the hot-leg of the thermosyphon (no subscript is used to distinguish u).

$$F_{visc} \cong -\frac{4\,L\,\rho_o\,A_{up}\,u}{(k_b/\nu)} \qquad (5)$$

Buoyant Force

The buoyant force can be developed by considering the difference in the hydrostatic pressure at the bottom of the thermosyphon due to lighter gas in the hot leg.

$$F_{buoy} = -\oint[\rho_o - \rho(T)]A\,\vec{g}\bullet d\vec{\ell} \qquad (6)$$

The temperature-dependent gas density is modeled using the Boussinesq approximation (neglecting the effect of the difference in molecular weights between vapor and air)

$$\rho(T) = \rho_o(1-\beta\Delta T) \qquad (7)$$

Eqns 6 and 7 show that the buoyant force is dictated by the vertical integral of the repository induced temperature change in the hot leg.

$$F_{buoy} = \rho_o\ g\ \beta\ A_{up}\int_{hot\,leg}\Delta T dz \qquad (8)$$

Given the observation that the gas has a negligible momentum in a porous medium, it is noted that the buoyant force (hence the buoyant gas flow) is in quasi-equilibrium with the evolving temperature field. Based on a review of more complicated calculations reported in the literature (Wang et. al., 1983; Pollock, 1986; Amter and Ross, 1991; Buscheck and Nitao 1992, 1993; Manteufel et al., 1993), it was found that the temperature profile is determined by conduction heat transfer. At early times (< 100 years) the increase in temperature is within the region between the water table and ground surface, and all of the radioactive decay heat goes into heating the medium (neglecting the energy removed by ventilation of the mined excavations). In this case, the vertical integral of the temperature profile is simply related to the time integral of the heat input

$$\int_{hot\,leg}\Delta T dz = \frac{1}{(\rho c)_{rock}}\int_{\tau=0}^{t} q_{src}\,d\tau \qquad (9)$$

Hence, the net buoyant force (from the combination of Eqns 8 and 9) is related to the time integral of the heat input:

$$F_{buoy} = \frac{\rho_o\,g\,\beta A_{up}}{(\rho c)_{rock}}\int_{\tau=0}^{t} q_{src}(\tau)\ d\tau \qquad (10)$$

Eqn 10 is an alternative expression for Eq 8, and is valid as long as the thermal energy only heats the rock in the unsaturated zone (i.e., is not removed by ventilation of the mined excavations, transferred into the medium below the water table, or convected into the atmosphere at the land surface).

Combined Equation

The viscous and buoyant forces (Eqns 5 and 8) can be combined into Eq 1 to yield the buoyancy-induced, steady-state gas velocity.

$$u = \frac{g\,\beta\,k_b\int\Delta T dz}{4\,\nu\,L} \qquad (11)$$

Equation 11 contains an important result in that an analytical velocity scale has been derived. This result shows that the buoyancy-driven gas velocity is linearly dependent on the integral of the increase in rock temperature, and the bulk gaseous permeability, k_b, among other parameters. The uncertainty in each of the parameters was investigated and it was found that the greatest uncertainty is for the bulk permeability which is currently estimated to be about 4 orders-of-magnitude (1 millidarcy < k_b < 10 darcy) with the majority of data covering two orders of magnitude (0.1 < k_b < 10 darcy) (LeCain and Walker, 1994) and being spatially variable. Hence, the variability in k_b is expected to be larger than for other parameters in Eqn 11. At this time, site characterization activities are expected to reduce the uncertainty in k_b, however, it is expected that spatial variability will always be present in the geologic system.

VAPOR TRANSFER

The buoyancy-driven gas flow is expected to affect vapor transfer by advecting the vapor (which is generated at the repository horizon) above the repository. Without buoyant flow, the gas is essentially stagnant and vapor will flow by molecular diffusion into cooler regions which are both above and below the repository. With buoyant flow, a larger fraction of the vapor will flow to regions above the repository and condense therein. In this section, the influence of buoyant gas flow on vapor transfer and groundwater redistribution is assessed.

A simplified model can be developed for a source/sink term for liquid water based on the model of vapor transfer and condensation/vaporization. The model will be applied near the center of the repository and in the vertical direction (hence we use z instead of ℓ for the spatial location). The conservation equation for liquid water can be written as

$$\frac{\partial(\rho_\ell \phi S_\ell)}{\partial t} = - \frac{\partial q_{m,w,\ell}}{\partial z} + Q_{c/v} \qquad (12)$$

and for water vapor as

$$\frac{\partial(\rho_v \phi S_g)}{\partial t} = - \frac{\partial(q_{m,w,g} + j_{m,w,g})}{\partial z} - Q_{c/v} \qquad (13)$$

where $Q_{c/v}$ is the vapor-to-liquid transfer term which appears in both equations. The accumulation of water vapor is typically negligible in comparison with the transport and source/sink terms, hence Eq 13 can be approximated as

$$Q_{c/v} \cong - \frac{\partial(q_{m,w,g} + j_{m,w,g})}{\partial z} \qquad (14)$$

Each term on the right-hand side of Eq 14 can be defined further.

Advective Term

The advective mass flux of water vapor is equal to vapor density times gas velocity

$$q_{m,w,g} = \rho_v u \qquad (15)$$

Three simplifying assumptions are introduced: (i) local thermodynamic equilibrium exists between the liquid and vapor, (ii) the local gas density is approximately the saturated vapor density (i.e., Kelvin's vapor pressure lowering effects are neglected), and (iii) the maximum temperature does not exceed the boiling temperature ($T_m < T_{boil}$). Thus, the gradient of the advective vapor flux is

$$\frac{\partial q_{m,w,g}}{\partial z} = u \frac{d\rho_v}{dT} \frac{dT}{dz} \qquad (16)$$

From Claperyon's equation (Wark, 1983), it can be shown that

$$\frac{d\rho_v}{dT} \cong \rho_v \frac{h_{fg} M_w}{RT^2} \qquad (17)$$

hence

$$\frac{\partial q_{m,w,g}}{\partial z} \cong u \rho_v \frac{h_{fg} M_w}{RT^2} \frac{dT}{dz} \qquad (18)$$

Diffusive Term

The diffusive flux of water vapor is given by Fick's law

$$j_{m,w,g} = -D \frac{\partial \rho_v}{\partial z} \qquad (19)$$

so that the gradient of the diffusive mass flux of water vapor is

$$\frac{\partial j_{m,w,g}}{\partial z} = \frac{\partial}{\partial z}\left(-D \frac{\partial \rho_v}{\partial z}\right) \qquad (20)$$

Although the diffusion coefficient, D, can be spatially variable, it is assumed uniform here. As a result, Eq 20 can be rewritten as

$$\frac{\partial j_{m,w,g}}{\partial z} \cong -\rho_v D \left(\frac{h_{fg} M_w}{RT^2}\right) \left[\left(\frac{h_{fg} M_w}{RT^2}\right)\left(\frac{dT}{dz}\right)^2 + \frac{d^2T}{dz^2}\right] \qquad (21)$$

Combined Terms

Combining Eqns 18 and 21 into Eq 14 yields

$$Q_{c/v} = -\rho_v \left(\frac{h_{fg} M_w}{RT^2}\right) \left\{u \frac{dT}{dz} - D\left[\left(\frac{h_{fg} M_w}{RT^2}\right)\left(\frac{dT}{dz}\right)^2 + \frac{d^2T}{dz^2}\right]\right\} \qquad (22)$$

A dimensionless equation for $Q_{c/v}$ can be derived as

$$\hat{Q}_{c/v} = -\left(\frac{\rho_v}{\rho_o}\right) \left[\left(\frac{Pe}{Vp}\right)\left(\frac{d\theta}{d\hat{z}}\right) - \left(\frac{d\theta}{d\hat{z}}\right)^2 - \left(\frac{1}{Vp}\right)\frac{d^2\theta}{d\hat{z}^2}\right] \qquad (23)$$

A new dimensionless group of variables is introduced for convenience and called the "vapor pressure number," Vp,

because it is approximately equal to the fractional difference in vapor pressure due to the increase in temperature.

$$Vp \equiv \frac{h_{fg} M_w}{R T^2} \Delta T_m = \frac{1}{P_v} \frac{dP_v}{dT} \Delta T_m \cong \frac{\Delta P_v}{P_v} \quad (24)$$

From Eqn 24, it should be noted that the vapor pressure number is proportional to the increase in temperature caused by the heat. From Claperyon's equation, the dimensionless vapor density is

$$\frac{\Delta \rho_v}{\rho_v} = \exp\left(\frac{Vp \ \theta}{1 + \frac{\theta \Delta T_m}{T_o}} \right) \quad (25)$$

For a linear temperature profile, the second derivative is zero (e.g., $\frac{d^2\theta}{d\hat{z}^2} = 0$), and the first derivative is constant

$$\frac{d\theta}{d\hat{z}} = \begin{cases} -1 & \text{above repository} \\ 1 & \text{below repository} \end{cases} \quad (26)$$

For a linear temperature profile, Eq 23 simplifies to

$$\hat{Q}_{c/v} = \begin{cases} \left(\frac{\rho_v}{\rho_o}\right)\left[1 + \left(\frac{Pe}{Vp}\right)\right] & \text{above repository} \\ \left(\frac{\rho_v}{\rho_o}\right)\left[1 - \left(\frac{Pe}{Vp}\right)\right] & \text{below repository} \end{cases} \quad (27)$$

The spatial dependence of $Q_{c/v}$ is due to ρ_v being temperature dependent (Eq 25) and the temperature being a function of location from the repository. Equation 27 is plotted in Figure 2 for different (Pe/Vp) numbers which represent different strengths of gas flow (assuming T_o = 40 C, ΔT_m = 60 C in Eqn 25 as representative of below boiling conditions). At (Pe/Vp) = 0.0, advective effects are negligible and the vapor flows away from the repository horizon (at z/L = 0) where it condenses ($Q_{c/v} > 0$) in equal proportions both above and below the repository horizon. It is noted that the repository horizon is modeled as a point source of water vapor.

The amount of condensation decreases rapidly with increasing distance from the repository. Natural convection inherently tends to create upward flow through the repository (as illustrated in Figure 1). As the flow rate increases (and therefore, Pe increases), more vapor condenses above the repository than below. This is expected as the bulk gas flow transports vapor from below and deposits it as condensate above the repository. This is the key effect (advection of vapor upward through repository) of the buoyant thermosyphon on groundwater redistribution.

At high flows (Pe/Vp > 1.0), the buoyant gas flow is predicted to be strong enough to dry out the medium below the repository ($Q_{c/v} < 0$) and significantly increase the amount of condensate above the repository. The criterion for when condensation no longer occurs below the repository is (Pe/Vp) > 1 which can be determined from Eq 27.

Buoyancy-driven advective gas flow affects vapor transfer when the combined vapor transport is larger than the diffusive-only transport (i.e., stagnant gas). To gauge the effect of buoyant gas flow on vapor transfer, the ratio of total vapor transfer (advective and diffusive) to the diffusive vapor transfer is calculated at a point just above the repository level

$$\left.\frac{j_{m,w,g} + q_{m,w,g}}{j_{m,w,g}}\right|_{\hat{z}=0^+} = 1 + \frac{\rho_v u}{D\left(\frac{\partial \rho_v}{\partial z}\right)} = 1 + \left(\frac{Pe}{Vp}\right) \quad (28)$$

In Figure 3, the relative strengths of diffusive and advective transport of vapor is compared for a range of Peclet number. In the figure, the ratio of (Pe/Vp) is an indication of the strength of advection and is plotted on the x-axis. The ratio of total mass flux of water vapor (advective and diffusive) to the diffusive mass flux (Eq 28) is an indication of the influence of gas flow on vapor transport, and is plotted on the y-axis. For a Peclet number near zero (indicating a stagnant gas), the vapor transfer is diffusion dominated. As the strength of the gas flow increases, the advective contribution becomes increasingly important, until at high values of Pe, the vapor transfer is dominated by advection. Three distinct regimes for vapor transfer can be identified:

- diffusion dominated (Pe/Vp < 0.1),
- both diffusion and advection important (0.1 < Pe/Vp < 1.0), and
- advection dominated (Pe/Vp > 1.0).

HEAT TRANSFER

The relative strengths of conductive and convective transport of thermal energy is compared in Figure 4. (It is noted that heat diffusion is frequently called conduction and heat advection is frequently called convection, so that these terms are used interchangeably.) The ratio of the total heat flux to the conductive component (through the rock mass), is plotted on the y-axis. The total

heat flux consists of three components, namely: (i) the conductive component (the negative sign in Fourier's law is neglected for convenience)

$$j_{e,cond} = k_{rock} \frac{dT}{dz} \tag{29}$$

(ii) the conductive component associated with the latent heat of the vapor (the negative sign in Fick's law is neglected)

$$j_{e,w,g} = h_{fg} D \frac{d\rho_v}{dz} \tag{30}$$

and (iii) the convective component associated with the latent heat of vapor

$$q_{e,w,g} = h_{fg} \rho_v u \tag{31}$$

The sensible heat of the air can be included, but it readily can be shown to be negligible (in comparison with other transport mechanisms) under the anticipated conditions at Yucca Mountain. The ratio of interest is

$$\frac{j_{e,cond} + q_{e,w,g} + j_{e,w,g}}{j_{e,cond}} = 1 + \frac{(h_{fg})^2 \rho_v D M_w}{k_{rock} R T^2} \left(\frac{Pe}{Vp} + 1 \right) \tag{32}$$

Based on typical values associated with the proposed repository (especially, k_{rock} ~ 2 W/(m-C)), one can compute

$$\frac{j_{e,cond} + q_{e,w,g} + j_{e,w,g}}{j_{e,cond}} \cong 1 + 10^{-2} \left(\frac{Pe}{Vp} + 1 \right) \tag{33}$$

Equation 33 is plotted in Figure 4. A number of conclusions can be drawn, the first being that the heat transfer associated with the diffusion of water vapor is always negligible compared with conduction through the geologic medium. The specific criterion for such a conclusion is:

$$\frac{j_{e,w,g}}{j_{e,cond}} << 1 \tag{34}$$

This ratio has been calculated to be approximately 10^{-2} so that conductive energy transport associated with the latent heat of vapor is negligible. Another conclusion is that the heat transfer is conduction dominated for low values of Pe/Vp and convection becomes more important at higher values of Pe/Vp. Three distinct regimes for heat transfer can be identified:

- conduction dominated (Pe/Vp < 10),
- both conduction and convection important (10 < Pe/Vp < 100), and
- convection dominated (Pe/Vp > 100).

The transition from conduction dominated to convection dominated occurs over a one decade change in Pe/Vp.

One of the more important conclusions of this work is that vapor transfer is more readily affected by buoyant gas flow than heat transfer. From these analyses, it is predicted that the threshold for advective effects is two decades lower for vapor transfer than for heat transfer. This conclusion is in agreement with the numerical calculations of Buscheck and Nitao (1992,1993).

VAPOR AND HEAT TRANSFER REGIMES

From these simple analyses, three regimes can be identified as illustrated in Figure 5. For Pe/Vp < 0.1, both heat and vapor transfer are diffusion-dominated and are not affected by buoyant gas flow. For 0.1 < Pe/Vp < 10, the buoyant gas flow has an effect on vapor transfer, yet has a negligible effect on heat transfer. For Pe/Vp > 10, buoyant flow has an effect on both vapor and heat transfer. In addition, best estimates are provided for the conditions at Yucca Mountain. It is important to restate many of the assumptions and approximations introduced in these analyses. Specifically, the current model:

- fails to account for vapor pressures greater than atmospheric pressure (i.e., boiling)
- neglects preferential flow paths in the geologic medium and assumes the flow patterns indicated in Figure 1
- neglects other sources of gas flow (e.g., topographic or barometric)
- neglects vapor pressure lowering and the development of a dry zone
- assumes local thermodynamic equilibrium for the water vapor

CONCLUSIONS

A simplified model for buoyancy-driven gas flow is developed based on a thermosyphon analysis (Figure 1), where it is concluded that:

- The upward buoyant gas velocity through the repository horizon is linearly proportional to bulk permeability and maximum repository temperature increase.
- There currently exists ~4 orders-of-magnitude uncertainty in the bulk permeability of the medium which overwhelms uncertainties in other parameters.

The effect of gas flow on vapor transfer is assessed (Figures 2 and 3), where it is concluded that:

- At low gas flow, the liquid which is vaporized at the repository horizon is distributed equally as condensate both above and below the repository horizon.
- At higher gas flow (Pe/Vp > 0.1), a larger fraction of the vapor condenses above the repository horizon.
- At very high gas flows (Pe/Vp > 1.0), the buoyant gas acts to dry out the medium below the repository and deposit the vapor as condensate above the repository.

The effect of gas flow on heat transfer is assessed (Figure 4), where it is concluded that:

- The heat transfer is diffusion (or conduction) dominated for Pe/Vp < 10.0, and advection (or convection) dominated for Pe/Vp > 100.0.

Three regimes of heat and vapor transfer are identified and distinguished by the Pe/Vp number (Figure 5).

- Regime I, with Pe/Vp < 0.1, where both vapor and heat transfer are diffusion dominated.
- Regime II, with 0.1 < Pe/Vp < 10.0, where gas flow has an effect on vapor transfer yet heat transfer is diffusion dominated.
- Regime III, with Pe/Vp > 10, where gas flow has an effect on both vapor and heat transfer.
- The vapor transfer is more readily affected by buoyant gas flow than heat transfer, by ~2 decades in the Pe/Vp number. This conclusion is in agreement with the results of numerical simulations.

ACKNOWLEDGMENTS

This paper was prepared to document work performed by the Center for Nuclear Waste Regulatory Analyses (CNWRA) for the U.S. Nuclear Regulatory Commission (NRC) under Contract No. NRC-02-88-005. The activities reported herein were performed on behalf of the NRC Office of Nuclear Regulatory Research, Division of Regulatory Applications. The report is an independent product of the CNWRA and does not necessarily reflect the views or regulatory position of the NRC.

REFERENCES

Amter, S., N. Lu, and B. Ross., 1991, Thermally Driven Gas Flow Beneath Yucca Mountain, Nevada. R.R. Eaton et al. (editors). *Multiphase Transport in Porous Media*, FED-122. American Society of Mechanical Engineers: 17-23.

Buscheck, T.A. and J.J. Nitao., 1992, The impact of thermal loading on repository performance at Yucca Mountain. *Proceedings of the International High-Level Radioactive Waste Management Conference*. La Grange Park, IL: American Nuclear Society: 1003-1017.

Buscheck, T.A. and J.J. Nitao., 1993, Repository-Heat-Driven Hydrothermal Flow at Yucca Mountain, Part I: Modeling and Analysis. *Nuclear Technology* 104: 418-448.

DOE (U.S. Department of Energy), 1993, Yucca Mountain Site Characterization Project, Reference Information Base 93-02, Rev 0.DOE Yucca Mountain Project Office.

LeCain G.D., and J.N. Walker, 1994, Results of Air-Permeability Testing in a Vertical Borehole at Yucca Mountain, Nevada. *Proceedings of the International High-Level Radioactive Waste Management Conference*. La Grange Park, IL: American Nuclear Society: (4) 2782-2788.

Manteufel, R.D. and M.W. Powell, 1994, Thermospyhon Analysis of a Repository: A Simplified Model for Vapor Flow and Heat Transfer. *Proceedings of the International High-Level Radioactive Waste Management Conference*. La Grange Park, IL: American Nuclear Society, 2207-2216.

Manteufel, R.D. and R.T. Green., 1993, Observations of Thermally-Driven Liquid Redistribution in a Partially Saturated Porous Medium. FED-173/HTD-265, R.R. Eaton et al. (eds), *MultiPhase Transport in Porous Media*. New York, NY: American Society of Mechanical Engineers.93-107.

Manteufel, R.D., M.P. Ahola, D.R. Turner, and A.H. Chowdhury., 1993, *A Literature Review of Coupled Thermal-Hydrologic-Mechanical-Chemical Processes Pertinent to the Proposed High-Level Nuclear Waste Repository at Yucca Mountain*. NUREG/CR-6021. Washington, DC: Nuclear Regulatory Commission.

Pollock D.W., 1986, Simulation of fluid flow and energy transport processes associated with high-level radioactive waste disposal in unsaturated alluvium. *Water Resources Research* 22(5): 765-775.

Pruess K., J.S.Y. Wang, and Y.W. Tsang, 1990a, On thermohydrologic conditions near high-level nuclear wastes emplaced in partially saturated fractured tuff. 1. Simulation studies with explicit consideration of fracture effects. *Water Resources Research* 26(6): 1235-1248.

Pruess K., J.S.Y. Wang, and Y.W. Tsang, 1990b, On thermohydrologic conditions near high-level nuclear wastes emplaced in partially saturated fractured tuff. 2. Effective continuum approximation. *Water Resources Research* 26(6): 1249-1261.

Rajen, G. and F.A. Kulacki, 1987, Experimental and Numerical Study of Natural Convection in a Porous Layer Locally Heated from Below - A Regional Laboratory Model for a Nuclear Waste Repository. HTD-67. E.B. McAssey, Jr and V.E. Schrock, eds. *Heat Transfer Problems in Nuclear Waste Management*, New York, NY: 19-26.

Rajen, G., 1989, *Buoyancy-Induced Flow and Heat Transfer in Porous and Fissured Media.* Ph.D. Thesis. University of Delaware.

Wang, J.S.Y., D.C. Mangold, R.K. Spencer, and C.F. Tsang. 1983, *Thermal impact of waste emplacement and surface cooling associated with geologic disposal of nuclear waste.* NUREG/CR-2910. Washington, DC: Nuclear Regulatory Commission.

Wark, K, 1983, *Thermodynamics*. New York, NY: McGraw-Hill).

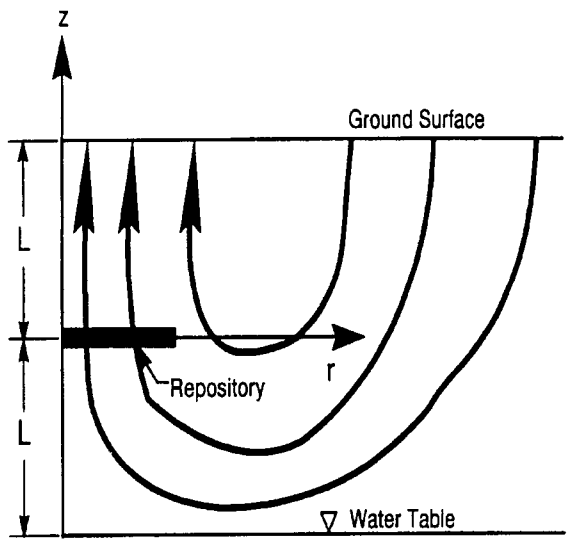

FIGURE 1. ANTICIPATED GAS STREAMLINES AT AN UNSATURATED REPOSITORY.

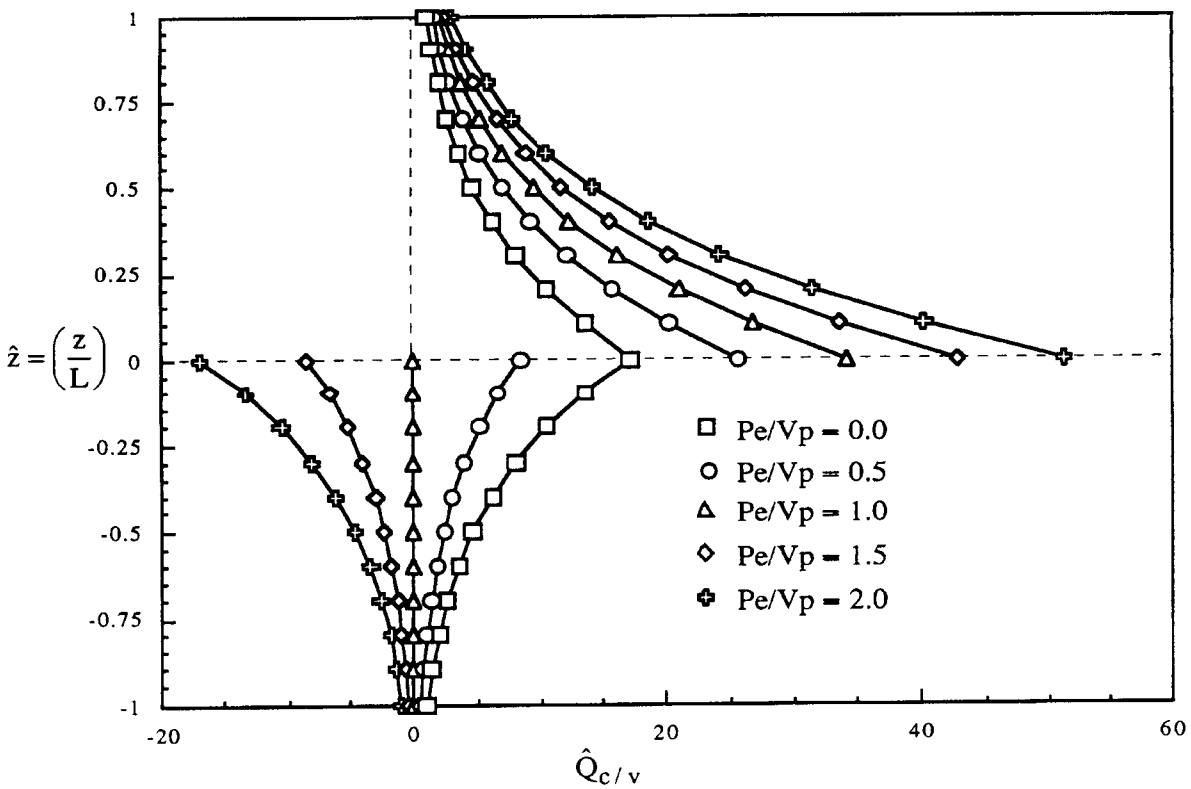

FIGURE 2. EFFECTS OF GAS FLOW ON THE CONDENSATION/VAPORIZATION SOURCE TERM.

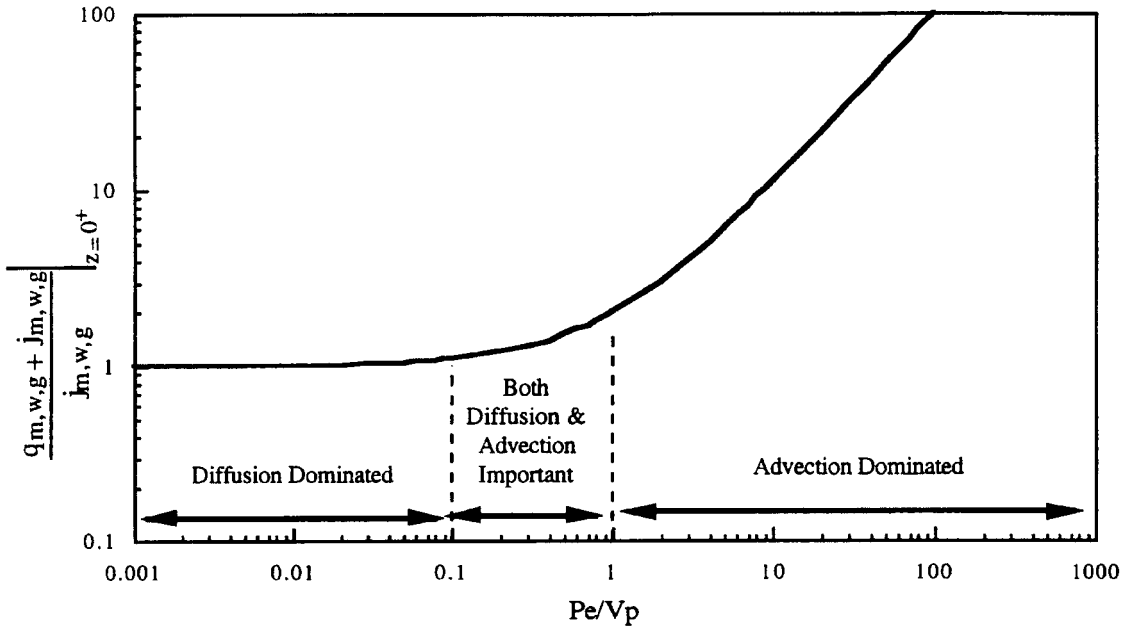

FIGURE 3. EFFECTS OF GAS FLOW ON VAPOR TRANSFER NEAR THE REPOSITORY.

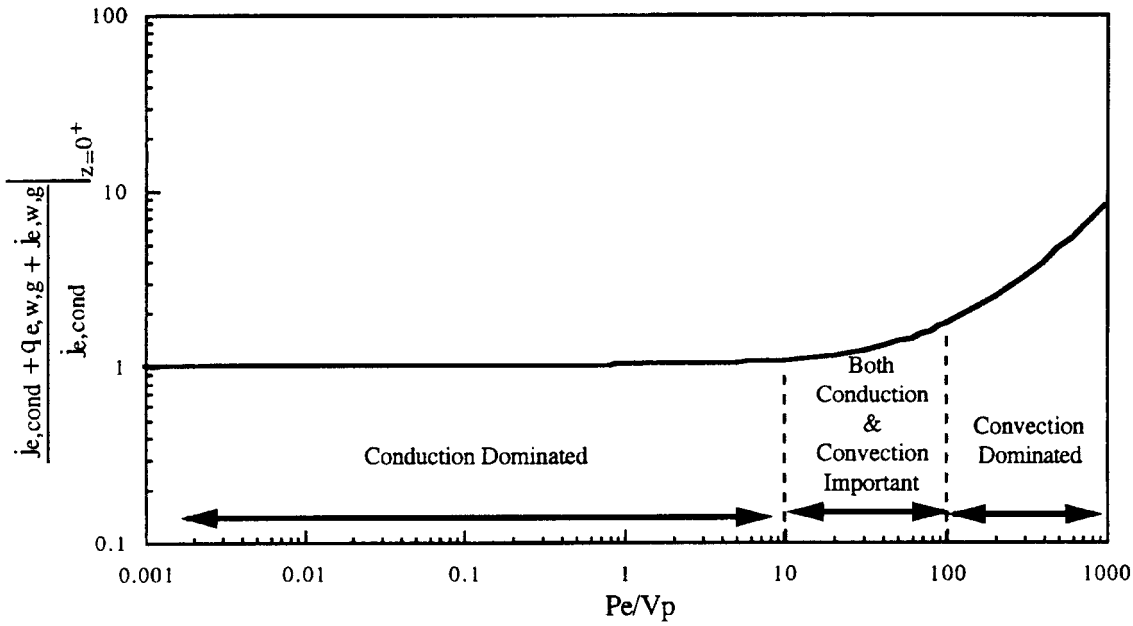

FIGURE 4. EFFECTS OF GAS FLOW ON HEAT TRANSFER NEAR THE REPOSITORY.

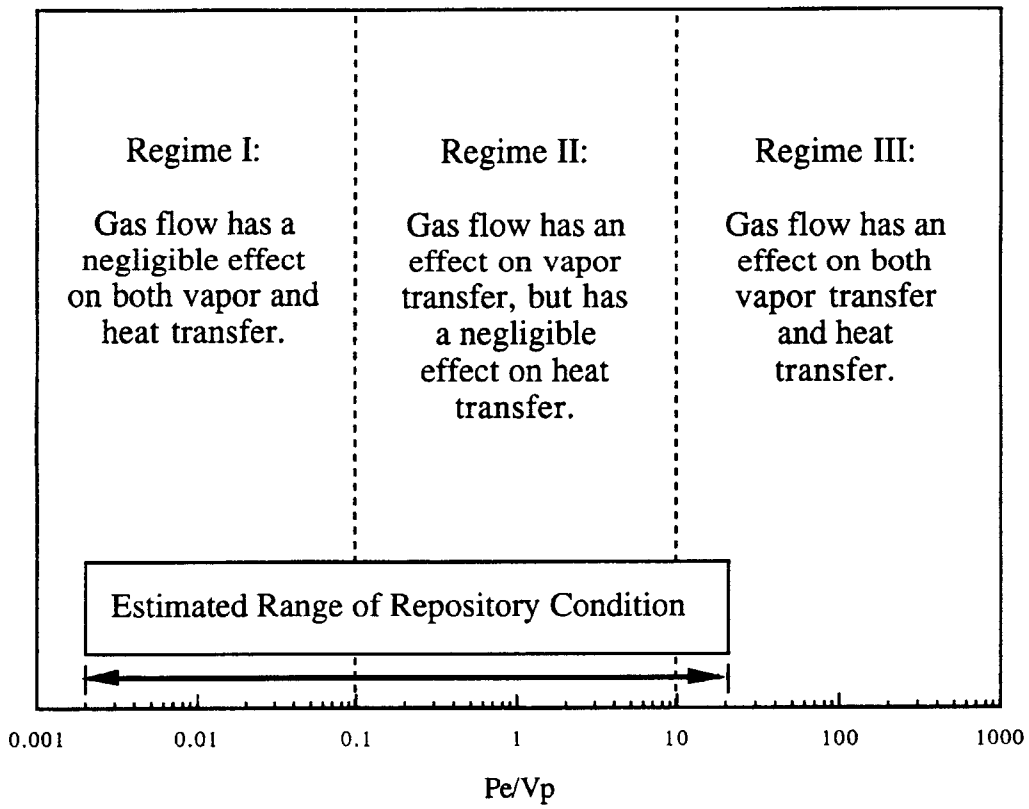

FIGURE 5. REGIMES OF VAPOR AND HEAT TRANSFER AS AFFECTED BY GAS FLOW.